

RESEARCH

Open Access

Joint DOD/DOA estimation in MIMO radar exploiting time-frequency signal representations

Yimin D Zhang^{1*}, Moeness G Amin¹ and Braham Himed²

Abstract

In this article, we consider the joint estimation of direction-of-departure (DOD) and direction-of-arrival (DOA) information of maneuvering targets in a bistatic multiple-input multiple-output (MIMO) radar system that exploits spatial time-frequency distribution (STFD). STFD has been found useful in solving various array processing problems, such as direction finding and blind source separation, where nonstationary signals with time-varying spectral characteristics are encountered. The STFD approach to array processing has been primarily limited to conventional problems for passive radar platform that deals with signal arrivals, while its use in a MIMO radar configuration has received much less attention. This paper examines the use of STFD in MIMO radar systems with application to direction finding of moving targets with nonstationary signatures. Within this framework, we consider the use of joint transmit and receive apertures for the improved estimation of both target time-varying Doppler signatures and joint DOD/DOA. It is demonstrated that the STFD is an effective tool in MIMO radar processing when moving targets produce Doppler signatures that are highly localized in the time-frequency domain.

Keywords: radar signal processing, MIMO radar, direction finding, joint DOD/DOA estimation, time-frequency analysis, moving target tracking

1. Introduction

Multiple-input multiple-output (MIMO) radar is an emerging technology that has attracted significant interest in the radar community [1,2]. By emitting orthogonal waveforms from the transmit array antennas and utilizing matched filterbanks in the receivers to extract the waveform components, MIMO radar systems can exploit the spatial diversity and the higher number of degrees of freedom to improve resolution, clutter mitigation, and classification performance. In particular, a monostatic MIMO radar system exploiting colocated array antennas can provide effective array designs to achieve an extended virtual aperture which becomes the sum coarray of the transmit array and the receive arrays [2,3]. A bistatic MIMO radar with respectively colocated transmit and receive array antennas, on the other hand, is capable of jointly estimating the direction-of-departure (DOD) and direction-of-arrival (DOA) of targets

[4-7]. There are various reasons motivating the use of bistatic radars, ranging from improving covertness to achieving improved location accuracy [8]. In the MIMO radar context, the combined DOD and DOA information allows triangulation of target locations. This is particularly important in narrowband radar systems, such as over-the-horizon radar, which do not have a high range resolution [9]. The joint transmit and receive beamforming offers improved interference/jamming cancellation capability, which can be performed without the need for a priori information at the transmitter. This is made possible since the transmit beamforming is performed at the receiver [10].

Radar signals are often nonstationary with Doppler frequencies that may change slowly or rapidly with time. This is the case of Doppler signatures that are generated due to target movement and maneuvering. For those nonstationary signals, time-frequency distributions (TFDs) have been widely used as a powerful tool for signal analysis, enhancement, and discrimination [11]. When used in array processing applications, time-frequency signal representations yield improved signature

* Correspondence: yimin.zhang@villanova.edu

¹Center for Advanced Communications, Villanova University, Villanova, PA 19085, USA

Full list of author information is available at the end of the article

detection, interference cancelation, direction estimation, and waveform recovery. In particular, the development of spatial time-frequency distribution (STFD) has led to a new paradigm for processing a large class of nonstationary signals in multi-sensor array applications [12-24].

The STFD is defined by the STFD matrix, which includes the auto-sensor TFDs along its diagonal and cross-sensor TFDs as off-diagonal elements. The STFD matrix is related to the source TFD matrix by the spatial mixing matrix in a manner similar to the commonly used formula in array processing problems using second-order statistics that relates the sensor spatial covariance matrix to the source covariance matrix. This similarity has enabled eigenstructure and subspace methods to play a role in high-resolution DOA estimation of nonstationary sources. It was shown in [19] that, by constructing an STFD matrix from the selected time-frequency points of highly localized signal energy, the corresponding signal and noise subspace estimates, as a result of signal-to-noise ratio (SNR) enhancement, become more robust to noise than their counterparts obtained using the data covariance matrix. In addition, the selected time-frequency points can pertain to a single or few sources, thus allowing the consideration of individual or subset of the sources in the field of view. The separability of the source time-frequency signature and the flexibility in time-frequency point set selection further increase the SNR and reduce the mutual interference between the signals, yielding improved subspace robustness. Further, it allows processing more sources than the number of sensors. A number of direction finding techniques have been developed within the STFD framework to take advantages of the above properties (e.g., [13-15,17,20]). These techniques have shown improved performance compared to their conventional DOA approach counterparts.

The merits of time-frequency based DOA estimation can only be materialized through the selection of appropriate time-frequency points in the construction of the STFD matrices. While in some scenarios the selection of peak time-frequency points may be relatively easy, the problem can be more challenging in other situations, e.g., when the signals are highly contaminated by noise. A typical radar return signal is very weak with a low SNR. Therefore, it becomes necessary to utilize the spatial diversity to enhance the time-frequency signature of the signals of interest in the absence of knowledge of their directions. A simple example for achieving this purpose is through averaging of the TFDs over all receive sensors [21]. The array averaged TFD also helps in identifying auto-term and cross-terms points [22,23].

In this article, we consider the exploitation of STFD in bistatic MIMO radar applications. The goal is to

examine whether and how certain key advantages of the STFD, as described above, are preserved in the context of MIMO radar and their dependency on the number of transmit and receive antennas in bistatic MIMO systems. In particular, we deal with two important issues. The first issue is the enhancement of auto-term TFDs in the presence of both cross-terms and noise to obtain reliable auto-term identification. The second issue is the joint DOD and DOA estimation within the time-frequency framework that allows target selection and discrimination through the proper selection of time-frequency regions. It becomes clear that cross-term reductions, due to the averaging operation of sensor TFDs, benefit from both transmit and receive array apertures, whereas the noise reduction is determined by the number of virtual antennas. It is shown that the joint DOD/DOA estimation performance is improved through time-frequency based target discrimination when a closely separated target is eliminated from the evaluation.

In the presence of multiple targets, a bistatic radar is required to properly pair the estimated DOD and DOA results. Several techniques have been developed to void or to automatically obtain pairing operation [5-7]. In this article, we develop our time-frequency domain DOD/DOA estimation technique based on the combined ESPRIT-MUSIC method [7], which only requires two decoupled one-dimensional direction finding operations where the DOD and DOA are automatically paired.

The remainder of this article is organized as follows. The MIMO radar signal model is introduced in Section 2. The concept of STFD is reviewed in Section 3. The capability of enhancing the auto-term TFD over cross-term TFD and noise through averaging over virtual sensors is addressed in Section 4. Section 5 presents the joint DOD and DOA estimation in the time-frequency framework. Simulation results, validating our analyses and discussion, are presented in Section 6.

The following notations are used in this article. A lower (upper) case bold letter denotes a vector (matrix). $E[\cdot]$ represents statistical mean operation. $(\cdot)^*$, $(\cdot)^T$, and $(\cdot)^H$ respectively denote complex conjugation, transpose, and conjugate transpose (Hermitian) operations. $\text{Re}(\cdot)$ represents the real part operation of a complex variable, vector or matrix. \otimes denotes the Kronecker product and \diamond denotes the Khatri-Rao product. I_n expresses the $n \times n$ identity matrix. $\text{Diag}(\mathbf{x})$ denotes a diagonal matrix using the elements of \mathbf{x} as its diagonal elements, $\text{diag}(\mathbf{X})$ a vector consisting of the diagonal elements of matrix \mathbf{X} , and $\text{vec}(\mathbf{X})$ a vectorized result of matrix \mathbf{X} . In addition, $\mathbb{C}^N \times \mathbb{C}^M$ denotes the complete set of $N \times M$ complex entries, $[\mathbf{a}]_n$ denotes the n th element of vector \mathbf{a} , and $[\mathbf{A}]_{m,n}$ denotes the (m, n) th element of matrix \mathbf{A} . δ_n

is the Kronecker delta function which equals to 1 when $n = 0$ and 0 otherwise.

2. Signal model

Consider a bistatic MIMO radar system consisting of N_t closely spaced transmit antennas and N_r closely spaced receive antennas. Denote $\mathbf{S} \in \mathbb{C}^{N_t \times T}$ as the narrowband waveform matrix which contains orthogonal waveforms to be transmitted from N_t antennas over a pulse-repetition period of T fast-time samples. We assume that the waveform orthogonality is achieved in the fast-time domain. That is, by denoting s_i as the i th row of matrix \mathbf{S} , s_i and s_j are orthogonal for any $i \neq j$ with different delays, and s_i is orthogonal to the delayed version of itself. We also assume that s_i has a unit norm, i.e., $\mathbf{S}\mathbf{S}^H = \mathbf{I}_{N_t}$.

Consider a far-field range cell where L point targets are present with DOD θ_l and DOA ϕ_l , where $l = 1, \dots, L$. Then, the signal data received at the receive array corresponding to the range cell over a pulse repetition period is expressed as the following $N_r \times T$ complex matrix,

$$\mathbf{X}(t) = \mathbf{A}_r \mathbf{\Gamma}(t) \mathbf{A}_t^H \mathbf{S} + \mathbf{N}(t), \quad (1)$$

where t is the slow time index, $\mathbf{A}_r = [\mathbf{a}_r(\phi_1), \dots, \mathbf{a}_r(\phi_L)]$ and $\mathbf{A}_t = [\mathbf{a}_t(\theta_1), \dots, \mathbf{a}_t(\theta_L)]$, with $\mathbf{a}_r(\phi_l) \in \mathbb{C}^{N_r \times 1}$ and $\mathbf{a}_t(\theta_l) \in \mathbb{C}^{N_t \times 1}$, respectively, denoting the receive steering vector corresponding to DOA ϕ_l and the transmit steering vector corresponding to DOD θ_l . In addition, $\mathbf{\Gamma}(t) = \text{Diag}[\gamma_1(t), \dots, \gamma_L(t)]$ where $\gamma_l(t) = \rho_l(t) e^{j2\pi\beta(f_{D,l}(t), t)}$ denotes the complex reflection coefficient of the l th target during the t th pulse repetition period. The complex reflection coefficient is a function of the radar cross section (RCS), represented by $\rho_l(t)$, and the phase term, denoted as $\beta(f_{D,l}(t), t)$, which depends on the Doppler frequency $f_{D,l}(t)$ of the slow time index t . Moreover, $\mathbf{N}(t) \in \mathbb{C}^{N_r \times T}$ is the additive noise matrix, whose elements are assumed to be independent and identically distributed (i.i.d.) complex Gaussian random variables with zero mean and variance σ_n^2 . To qualify expression (1), it is assumed that the steering vectors remain unchanged during the entire slow-time processing period, which is often the case for far-field targets. The nonstationary signatures are a result of the target maneuvering, represented by the Doppler frequency $f_{D,l}(t)$.

The time-frequency analysis exploited in this article performs the best when the Doppler signatures are highly localized in the time-frequency domain and are represented by their respective instantaneous frequencies (IFs). For this reason, the RCS fluctuation is required to be constant or slowly time-varying. In this

article, we assume scan-by-scan RCS fluctuation (e.g., Swerling target models 1, 3, or 0) [25], such that the RCS remains invariant during certain processing time (e.g., a scan) or over the window length of the time-frequency kernel (as described in the following section).

By post-multiplying (1) by \mathbf{S}^H and utilizing the orthogonality of the transmitted waveforms, we obtain $\mathbf{Y}(t) \in \mathbb{C}^{N_t \times N_r}$ as

$$\mathbf{Y}(t) = \mathbf{A}_r \mathbf{\Gamma}(t) \mathbf{A}_t^H + \mathbf{Z}(t), \quad (2)$$

where $\mathbf{Z}(t) = \mathbf{N}(t)\mathbf{S}^H$. Vectorizing $\mathbf{Y}(t)$ in (2) yields the following $N_t N_r \times 1$ vector

$$\mathbf{y}(t) = \mathbf{w}(t) + \mathbf{z}(t) = \mathbf{A}\mathbf{\gamma}(t) + \mathbf{z}(t), \quad (3)$$

where $\mathbf{w}(t) = \mathbf{A}\mathbf{\gamma}(t)$ is the noise-free portion of the signal vector,

$$\mathbf{A} = \mathbf{A}_t \diamond \mathbf{A}_r = [\mathbf{a}_1^{[t]} \otimes \mathbf{a}_1^{[r]}, \dots, \mathbf{a}_L^{[t]} \otimes \mathbf{a}_L^{[r]}], \quad (4)$$

with $\mathbf{a}_l^{[t]}$ and $\mathbf{a}_l^{[r]}$ denoting the l th column of \mathbf{A}_t and \mathbf{A}_r , respectively. In addition, $\gamma(t) = \text{diag}(\mathbf{\Gamma}(t)) = [\gamma_1(t), \dots, \gamma_L(t)]^T$, and $\mathbf{z}(t) = \text{vec}(\mathbf{Z}(t))$.

The noise component corresponding to the m th transmit waveform and the n th receive antenna is given by $z_{n,m}(t) = [\mathbf{z}(t)]_{(m-1)N_r+n} = \tilde{\mathbf{n}}_n(t) \tilde{\mathbf{s}}_m^H$, where $\tilde{\mathbf{n}}_n(t)$ is the n th row of the receive noise matrix $\mathbf{N}(t)$, and $\tilde{\mathbf{s}}_m$ is the m th row of waveform matrix \mathbf{S} , $m = 1, \dots, N_t$ and $n = 1, \dots, N_r$. Notice that we used (\cdot) to emphasize a row vector. It is clear that vector $\mathbf{z}(t)$ has a zero mean, spatially white across the virtual sensors, and its covariance matrix can be shown to be $\sigma_n^2 \mathbf{I}_{N_t N_r}$ because

$$\begin{aligned} \mathbb{E}[z_{n_1, m_1}(t) z_{n_2, m_2}^*(t)] &= \mathbb{E}[\tilde{\mathbf{n}}_{n_1}(t) \tilde{\mathbf{s}}_{m_1}^H (\tilde{\mathbf{n}}_{n_2}(t) \tilde{\mathbf{s}}_{m_2}^H)^*] \\ &= \mathbb{E}[\tilde{\mathbf{s}}_{m_2} \tilde{\mathbf{n}}_{n_2}^H(t) \tilde{\mathbf{n}}_{n_1}(t) \tilde{\mathbf{s}}_{m_1}^H] = \sigma_n^2 \delta_{n_1-n_2} \delta_{m_1-m_2}. \end{aligned} \quad (5)$$

3. Spatial time-frequency distribution

The concept of STFD was developed in the context of the evaluation of quadratic TFDs to account for nonstationary signals in a multi-sensor environment. STFD has solved various array signal processing problems, including direction finding, blind source separation, and signal recovery [12-23].

Assume that the time-frequency analysis takes place after waveform decompression. Therefore, the nonstationarity only accounts for the targets' Doppler signature over the slow-time domain. In typical radar applications, Doppler frequencies due to target maneuvering are much smaller than the carrier frequency, i.e., the slow-time waveforms can be considered to be narrowband. Then, the discrete version of the Cohen's class of auto-term quadratic TFD of signal $x(t)$ is defined as [26]

$$D_{xx}(t, f) = \sum_{u=-\infty}^{\infty} \sum_{\tau=-\infty}^{\infty} g(u, \tau) x(t+u+\tau) x^*(t+u-\tau) e^{-j4\pi f\tau}, \quad (6)$$

where $g(u, \tau)$ is the kernel function. Different kernel functions are used to generate TFDs with prescribed and desirable properties. For example, the pseudo Wigner-Ville distribution (PWVD), which is used later in our simulations, exploits $g(u, \tau) = \delta_u w(\tau)$ as its kernel, where $w(\tau)$ is a time-lag window function. In particular, the PWVD of $x(t)$ with a rectangular window of length H is expressed as

$$D_{xx}(t, f) = \sum_{\tau=-(H-1)/2}^{(H-1)/2} x(t+\tau) x^*(t-\tau) e^{-j4\pi f\tau}. \quad (7)$$

Similarly, the cross-term TFD between two signals $x(t)$ and $y(t)$ is defined as

$$D_{xy}(t, f) = \sum_{u=-\infty}^{\infty} \sum_{\tau=-\infty}^{\infty} g(u, \tau) x(t+u+\tau) y^*(t+u-\tau) e^{-j4\pi f\tau}. \quad (8)$$

Based on the above definitions of auto-term and cross-term TFDs, the discrete version of the quadratic STFD matrix of signal vector $y(t)$ can be defined as [12,24]

$$D_{yy}(t, f) = \sum_{u=-\infty}^{\infty} \sum_{\tau=-\infty}^{\infty} g(u, \tau) y(t+u+\tau) y^H(t+u-\tau) e^{-j4\pi f\tau}, \quad (9)$$

where $[D_{yy}(t, f)]_{m,n} = D[y]_m[y]_n^H(t, f)$. The diagonal elements of $D_{yy}(t, f)$ represent the auto-sensor TFD terms of the data corresponding to the same receiver and transmit waveform, whereas the off-diagonal elements are cross-sensor TFD terms between the data corresponding to different virtual sensors.

Notice that the term auto-term may in general refer to either auto-sensor TFD term or auto-component TFD term. To avoid confusion, we use the terminology auto-sensor term and cross-sensor term to emphasize how to distinguish them from auto-target term and cross-target term. We simply use auto-term and cross-term to refer to the latter.

Substituting (3) into the above expression, we obtain

$$D_{yy}(t, f) = \mathbf{A} D_{\gamma\gamma}(t, f) \mathbf{A}^H + \mathbf{A} D_{\gamma z}(t, f) + \mathbf{D}_{zy}(t, f) \mathbf{A}^H + \mathbf{D}_{zz}(t, f). \quad (10)$$

In the above expression, the first term in the right-hand side (RHS) represents the contribution from the target returns, whereas the second and third terms at the RHS are the interaction between the target return and noise, and the last term at the RHS is the auto-term of the noise vector. Note that the time-frequency analysis maps one-dimensional (1D) time-domain signals into two-dimensional (2D) time-frequency domain signal representations. For target signal return whose Doppler signature follows an IF law, the respective auto-term TFD concentrates the

signal energy around the IF. On the other hand, the energy of the last three terms spreads over the entire time-frequency domain. As a result, the effective signal-to-noise ratio (SNR) of the target signal returns, when evaluated at the time-frequency regions around the signal IFs, can be substantially improved. This property improves not only signal detection and Doppler signature classification in noisy environment, but also signal subspace estimation and robustness [15,19]. In addition, since the above expression is satisfied for all time-frequency points, the STFD matrix can be evaluated using time-frequency regions which only include a subset of signal returns, thus allowing better signal selection and discriminations for the joint DOD/DOA estimations.

Under the standard uncorrelated signal and noise assumption and the zero-mean white noise property, the expectation of the cross-term STFD matrices between the signal and noise vectors is zero, and it follows

$$E[D_{yy}(t, f)] = \mathbf{A} D_{\gamma\gamma}(t, f) \mathbf{A}^H + \sigma_n^2 \mathbf{I}_{N_r N_r}. \quad (11)$$

Equation (11) shows that the STFD matrix has a similar relationship to the covariance matrix which commonly arises in array processing based on second-order statistics. It is clear, therefore, that the subspace spanned by the principle eigenvectors of D_{yy} constructed over a selected time-frequency region Ω_0 is identical to that spanned by the columns of \mathbf{A}_0 , where \mathbf{A}_0 denotes a subset of \mathbf{A} corresponding to the columns whose corresponding signal components are included in the selected time-frequency region Ω_0 (in particular, $\mathbf{A}_0 = \mathbf{A}$ when all the target signals are included in the selected time-frequency region Ω_0). This fact implies that, when dealing with nonstationary signals, various array processing techniques can be straightforwardly applied in the time-frequency framework to take advantages of signal enhancement and source discrimination, as described above, which stem from the non-stationary properties of $\gamma(t)$.

4. Time-frequency averaging over virtual sensors

As evident from the above discussion, the selection of time-frequency region with high signal concentration amounts to SNR enhancement. Inclusion of time-frequency regions with only noise or weak signal presence in direction finding, on the other hand, will reduce the effective SNR and degrade the performance. Therefore, it is important to properly identify and select the auto-term TFD regions for target selection/discrimination and SNR enhancement, so as to improve DOD/DOA estimation performance. It has been shown in [19] that SNR enhancement gained in the time-frequency domain is particularly important for data with relatively low signal power, whereas target time-frequency signature discrimination is critical when the targets are closely

separated in the spatial domain. For both cases, time-frequency point selections should be performed prior to the DOD/DOA estimations.

In this section, we examine the enhancement of the auto-term TFDs of the target signals relative to noise and cross-term interference by averaging the auto-sensor TFD obtained at each virtual antenna. This averaging is considered an effective technique for the identification of auto-term and cross-term regions [21-23]. In the following two subsections, the effect of time-frequency averaging is analyzed from the MIMO radar perspective in two aspects, namely, the auto-term TFD enhancement over the cross-term TFD and the signal TFD enhancement over the noise.

4.1. Autoterm TFD enhancement over crossterm

In this subsection, we focus on the auto-term enhancement in the presence of cross-terms. Therefore, the presence of noise is ignored. The effect of noise is considered in the following subsection.

Mathematically, averaging the TFDs obtained at each array sensor amounts to taking the trace of the STFD matrix [18,22,23]. The diagonal elements of $\mathbf{D}_{yy}(t, f)$ represent the auto-terms of the signals received at the $N_t N_r$ virtual antennas, whereas the off-diagonal elements represent the cross-terms between them. For most commonly used time-frequency kernels, the auto-terms are real. These terms are also positive for meaningful time-frequency points where the signal energy is concentrated. On the other hand, cross-terms are complex in general, and their values depend on the relative phase between the contributing signals. As such, averaging TFDs over different antennas enhances the auto-terms, whereas the cross-terms are significantly suppressed if the spatial correlation between the contributing signals is low.

With the focus on cross-term suppression, we consider a noise-free scenario, where the i th diagonal element of $\mathbf{D}_{ww}(t, f)$, in the presence of L targets, is expressed as

$$\bar{D}_{w_i w_i}(t, f) = \sum_{l=1}^L \sum_{k=1}^L a_{il} a_{ik}^* D_{\gamma_l \gamma_k}(t, f), \quad (12)$$

where a_{il} is the (i, l) th element of \mathbf{A} . Averaging the $N_t N_r$ diagonal elements of $\mathbf{D}_{ww}(t, f)$ thus becomes

$$\bar{D}_{ww}(t, f) = \frac{1}{N_t N_r} \sum_{i=1}^{N_t N_r} D_{w_i w_i}(t, f) = \sum_{l=1}^L \sum_{k=1}^L \beta_{l,k} D_{\gamma_l \gamma_k}(t, f), \quad (13)$$

where

$$\beta_{l,k} = \frac{1}{N_t N_r} \sum_i a_{il} a_{ik}^* \quad (14)$$

is the spatial correlation, defined in the virtual array of $N_t N_r$ sensors, of the return signals from targets l and k .

Using relationship (4), we can readily express the above result as

$$\beta_{l,k} = \beta_{l,k}^{[t]} \beta_{l,k}^{[r]}, \quad (15)$$

where

$$\beta_{l,k}^{[t]} = \frac{1}{N_t} [\mathbf{a}_k^{[t]}]^H \mathbf{a}_l^{[t]} \quad \text{and} \quad \beta_{l,k}^{[r]} = \frac{1}{N_r} [\mathbf{a}_k^{[r]}]^H \mathbf{a}_l^{[r]} \quad (16)$$

are, respectively, the spatial correlations of the two return signals defined in the transmit and receive arrays.

From the above discussion, it is clear that an MIMO radar enjoys significant advantages for cross-term suppressions. The fact that cross-terms are attenuated by the product of the spatial correlations defined in both transmit and receive arrays makes MIMO radar very attractive. Therefore, effective cross-term suppression may be achieved when either the transmitter or the receiver, or both, has a low spatial correlation.

4.2. Signal TFD Enhancement over Noise

From (3), we can write the signal received at the i th array sensor as

$$y_i(t) = w_i(t) + z_i(t). \quad (17)$$

The auto-sensor term TFD of the above signal, which is the i th diagonal element of \mathbf{D}_{yy} , is expressed as

$$D_{y_i y_i}(t, f) = D_{w_i w_i}(t, f) + D_{w_i z_i}(t, f) + D_{z_i w_i}(t, f) + D_{z_i z_i}(t, f). \quad (18)$$

The first term at the RHS in the above expression is the deterministic term, which has been discussed in detail in the previous subsection. The second and third terms are the cross-terms between the target signal and the noise, which obviously follow zero-mean complex Gaussian distributions with their variance independent of the sensor indices. The last term follows the chi-square distribution.

Averaging the auto-sensor terms over all virtual sensors, we obtain

$$\begin{aligned} \bar{D}_{yy}(t, f) &= \frac{1}{N_t N_r} \sum_{i=1}^{N_t N_r} D_{y_i y_i}(t, f) \\ &= \bar{D}_{ww}(t, f) + \frac{1}{N_t N_r} \sum_{i=1}^{N_t N_r} D_{w_i z_i}(t, f) \\ &\quad + \frac{1}{N_t N_r} \sum_{i=1}^{N_t N_r} D_{z_i w_i}(t, f) + \frac{1}{N_t N_r} \sum_{i=1}^{N_t N_r} D_{z_i z_i}(t, f). \end{aligned} \quad (19)$$

Because the noise is independent at each virtual sensor, the second and third terms in the RHS remain zero-mean complex Gaussian and their variance is reduced by a factor of $N_t N_r$. For a large number of $N_t N_r$, the last term can also be considered as complex

Gaussian as a result of the central limit theorem, with mean σ_n^2 , and its variance is reduced by a factor of $N_t N_r$ as well. As a result, the perturbation due to noise reduces as $N_t N_r$ increases, asymptotically leading to convergence to the expected value of $\bar{D}_{ww}(t, f) + \sigma_n^2$ as $N_t N_r$ goes to infinity.

5. Joint DOD and DOA estimations in the time-frequency framework

In bistatic radars, the DOD and DOA information can be synthesized to locate targets. For multiple targets, the combination of estimated DOD and DOA yields to a pairing ambiguity. Several techniques have been developed to void or to automatically obtain pairing operation [5-7]. These approaches, based on ESPRIT, or combined ESPRIT-MUSIC, can be extended to the time-frequency framework. We consider, as an example, the combined ESPRIT-MUSIC technique developed in [7] which only requires two decoupled 1D direction finding operations, where the DOD and DOA are automatically paired. In this section, we extend this technique into the spatial time-frequency framework. The DODs of the targets are first estimated using the time-frequency ESPRIT [20] and their DOAs are then obtained using time-frequency MUSIC [13]. To apply the ESPRIT-based method, both arrays are assumed to be uniform and linear, but the interelement spacings of the two arrays, respectively, denoted as d_t and d_r , may differ.

Consider a time-frequency region Ω_0 that contains signal returns from $L_0 \leq L$ targets. An STFD matrix, denoted as $D_{yy}(\Omega_0)$, can be obtained through weighted average of the STFD matrices across region Ω_0 , i.e.,

$$D_{yy}(\Omega_0) = \sum_{(t,f) \in \Omega_0} w(t, f) D_{yy}(t, f), \quad (20)$$

where $w(t, f)$ is the weighting coefficients, which can be chosen to be equal or proportional to the TFD magnitude. The signal subspace of matrix $D_{yy}(\Omega_0)$ corresponds to the L_0 target signals contained in the selected time-frequency region Ω_0 . In other words, it spans the same subspace as A_0 , where $A_0 = A_{0,t} \diamond A_{0,r}$ is a $N_t N_r \times L_0$ submatrix of A that contains the L_0 columns of matrix A , corresponding to the L_0 signals included in the selected time-frequency region.

Performing an eigen-decomposition of $D_{yy}(\Omega_0)$ and denoting $U_{s,0}$ as its $N_t N_r \times L_0$ signal subspace, whereas $U_{n,0}$ as the $N_t N_r \times (N_t N_r - L_0)$ noise subspace^a. Then, $U_{s,0}$ and A_0 are related by an unknown transformation matrix T as

$$U_{s,0} = A_0 T. \quad (21)$$

Divide the virtual array into two overlapping subarrays, respectively consisting of the first and last $(N_t - 1) N_r$ virtual antennas. Denote $A_{0,t}^{(1)}$ and $A_{0,t}^{(2)}$ as the first and last $N_t - 1$ rows of $A_{0,t}$, and let $A_0^{(t1)} = A_{0,t}^{(1)} \diamond A_{0,r}$ and $A_0^{(t2)} = A_{0,t}^{(2)} \diamond A_{0,r}$. Further, denote the averaged STFD matrices defined in these subarrays as $D_{yy}^{(1)}(\Omega_0)$ and $D_{yy}^{(2)}(\Omega_0)$, respectively. Then, their signal subspaces respectively relate to $A_0^{(t1)}$ and $A_0^{(t2)}$ through

$$U_{s,0}^{(1)} = A_0^{(t1)} T, \quad U_{s,0}^{(2)} = A_0^{(t2)} T. \quad (22)$$

$A_{0,t}^{(2)}$ and $A_{0,t}^{(1)}$ differ due to the antenna position and thus are related by

$$A_0^{(t2)} = A_0^{(t1)} \Phi_{[t]}, \quad (23)$$

where $\Phi_{[t]}$ is a diagonal matrix with diagonal elements $[\Phi_{[t]}]_{i,i} = \exp(j2\pi d_t \sin(\theta_i)/\lambda)$, $i = 1, \dots, L_0$. Similarly, $U_{s,0}^{(1)}$ and $U_{s,0}^{(2)}$ are related by

$$U_{s,0}^{(2)} = U_{s,0}^{(1)} \Psi_{[t]}. \quad (24)$$

From the above results, $\Psi_{[t]}$ can be obtained from $U_{s,0}^{(1)}$ and $U_{s,0}^{(2)}$. Substituting (23) into (24), we obtain

$$U_{s,0}^{(1)} = A_0^{(t1)} T, \quad U_{s,0}^{(2)} = A_0^{(t1)} \Phi_{[t]} T. \quad (25)$$

Therefore, it is concluded from (24) and (25) that $\Psi_{[t]}$ and $\Phi_{[t]}$ are related by $\Psi_{[t]} = T^{-1} \Phi_{[t]} T$, that is, $\Phi_{[t]}$ can be obtained as the eigenvalues of $\Psi_{[t]}$. As such, the DODs θ_i can be obtained for $i = 1, \dots, L_0$.

To estimate the DOAs after DODs are obtained, the ESPRIT-MUSIC method is based upon the fact that the noise subspace and the steering vector of the virtual array are orthogonal [7]. In the time-frequency framework, this leads to a time-frequency MUSIC based approach for each estimated θ_i , $i = 1, \dots, L_0$, i.e., estimating the paired ϕ_i by finding the peaks of the following pseudo spatial spectrum

$$f(\phi) = \frac{1}{a_r^H(\phi) [a_t(\theta_i) \otimes I_{N_r}]^H U_{n,0} U_{n,0}^H [a_t(\theta_i) \otimes I_{N_r}] a_r(\phi)}. \quad (26)$$

When the receive array is uniform linear, for which the receive steering vector can be expressed as a polynomial function of $z = \exp(-j2\pi d_r \sin(\phi)/\lambda)$, i.e.,

$$a_r(\phi) = [1, e^{-\frac{j2\pi d_r}{\lambda} \sin(\phi)}, \dots, e^{-\frac{j2\pi (N_r-1)d_r}{\lambda} \sin(\phi)}]^T = [1, z, \dots, z^{N_r-1}]^T, \quad (27)$$

the paired DOA ϕ_i can be solved using the simpler time-frequency root-MUSIC approach that finds the root inside and closest to the unit circle of the following

polynomial

$$\mathbf{a}_r^H(\phi)[\mathbf{a}_t(\theta_i) \otimes \mathbf{I}_{N_r}]^H \mathbf{U}_{n,0} \mathbf{U}_{n,0}^H [\mathbf{a}_t(\theta_i) \otimes \mathbf{I}_{N_r}] \mathbf{a}_r(\phi) = 0. \quad (28)$$

For the directions of other $L - L_0$ targets, the same procedure can be carried out in different time-frequency regions where these signals are included.

By exploiting target selection/discrimination through a time-frequency region selection, significant performance improvement can be achieved, particularly in the challenging situations such that multiple targets are closely spaced in angle but are separable in the time-frequency domain. Specifically, when a time-frequency region with a single target present can be identified, the DOD and DOA can be estimated with simple phase examinations, and no pairing operation is needed.

6. Simulation results

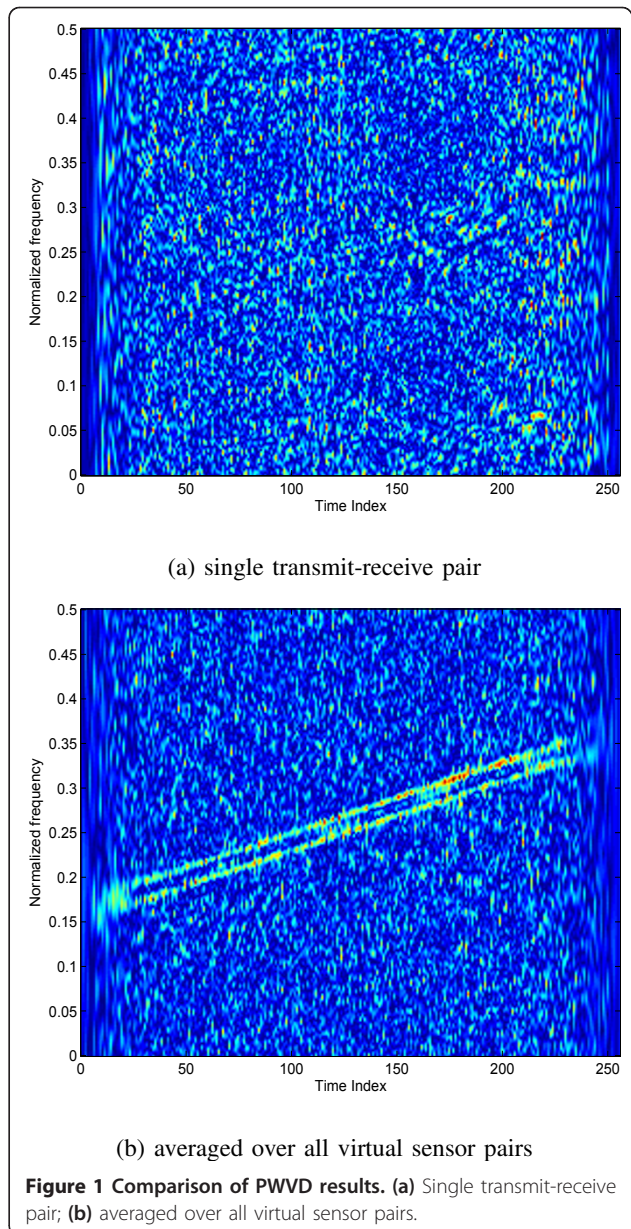
Consider a scenario in which two moving targets appear in a specific range bin of interest. The bistatic radar consists of a linear transmit array consisting of $N_t = 4$ antennas and a linear receive array consisting of $N_r = 6$ antennas. The transmit and receive arrays are assumed to be distantly separated. Half wavelength interelement spacing is set for both transmit and receive arrays. The waveforms transmitted from different transmit antennas are considered orthogonal, and the cross-correlation between different transmit waveforms is ignored. The total number of slow-time samples is 256 for each waveform. The RCS is considered constant over the entire 256 slow-time samples. The noise at each virtual sensor are assumed to be i.i.d., and the input SNR of all the return signals are assumed to be identical.

Two different examples are simulated in this section. In the first example, the two targets have close DODs (10° and 15°) observed at the transmitter, whereas their DOAs observed at the receiver have a larger separation (5° and 20°). The parameters of the targets are summarized in Table 1. The increasing Doppler signature of each target indicates the target movement towards the transmit and receive arrays in a way that the sum two-way slant range decreases over time.

In Figure 1a we depict the PWVD of the signal corresponding to the first receive antenna and the waveform transmitted from the first transmit antenna. The PWVD averaged over all the $N_t N_r = 24$ transmit and receive antenna combinations is shown in Figure 1b. The input SNR in this plot is -12 dB. To reduce the sidelobe

Table 1 Signal parameters of Example 1

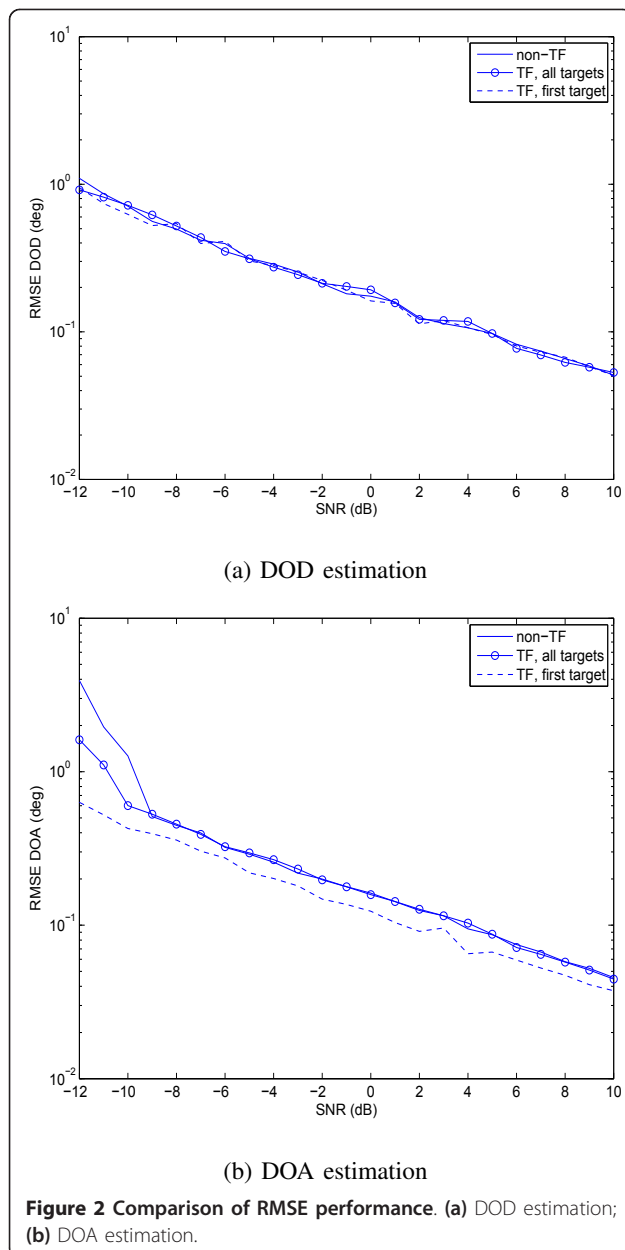
	Start freq.	End freq.	DOD (deg)	DOA (deg)
Target 1	0.15	0.35	10	5
Target 2	0.17	0.37	15	20



interference, a Hamming window of length $H = 127$ is used in computing the PWVD. It is evident that, while the TFD auto-terms of the signals are difficult to be recognized in the single transmit-receive antenna pair case because of the presence of a high level of noise, they become clearly identifiable in the sensor averaged TFD due to substantial mitigation of the noise as well as the cross-terms. As discussed in Section 5, cross-terms in the averaged TFD are attenuated according to the varying level of spatial correlation between the respective contributing signal components, whereas the reduction of the noise primarily depends on the number of virtual sensors. The latter, in our case, is the product of the number of transmit antennas and the number of

receive antennas. In this example, the spatial correlation coefficient has a high value of 0.956 at the transmit array and a low value of 0.288 at the receive array, resulting in an overall spatial correlation coefficient of the MIMO array at a low level of 0.275 that results in good cross-term suppression. It is noted that, because of the significant cross-term suppression, owing to spatial domain filtering, the two close chirp waveforms can be clearly separated in the time-frequency domain for IF estimation and target discrimination.

In Figure 2, the root-mean-square error (RMSE) of the DOD and DOA estimation results of the first target are compared for three different scenarios, namely, joint



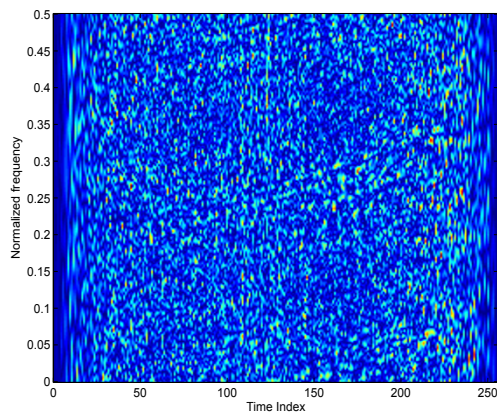
ESPRIT-MUSIC without the use of time-frequency analysis, time-frequency ESPRIT-MUSIC with all three signals selected for consideration, and time-frequency ESPRIT-MUSIC that only considers the signal corresponding to the first target. The results are averaged over 100 independent trials. When both signals are selected in the time-frequency ESPRIT-MUSIC, the performance is almost the same as the conventional ESPRIT-MUSIC when the input SNR is moderate or high. While the time-frequency ESPRIT-MUSIC benefits from the SNR enhancement, the performance is nevertheless affected by colored noise due to the selection of time-frequency regions. As has been the case in time-frequency DOA estimation techniques [15,19], the advantage of utilizing time-frequency analysis becomes more pronounced in the underlying example in low SNR scenarios, where the higher-order error terms becomes dominant in the conventional ESPRIT-MUSIC technique. It is interesting to note that, because of the wider separations of the targets in terms of their DOAs, good DOD estimation performance is achieved despite of the small angular separation of the two DODs. Further, by selecting only the first target for joint DOD/DOA estimation through the time-frequency domain discriminations, the DOA estimation performance is substantially improved, whereas the improvement of the DOD estimation performance is fairly modest.

In the second example, the two targets have close DODs (10° and 15°) and close DOAs (15° and 20°). The parameters of the targets are summarized in Table 2. As seen below, the effect of cross-terms in this case is more significant. Therefore, we use two signals of larger Doppler frequency difference so as to avoid the effect of cross-terms in auto-term selections.

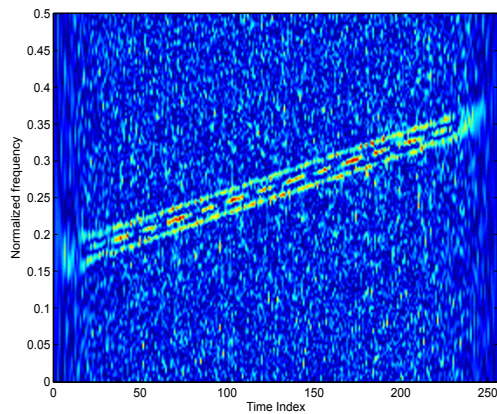
In Figure 3a we depict the PWVD of the signal corresponding to the first receive antenna and the waveform transmitted from the first transmit antenna. The Hamming window of length 127 remains the same as in the previous example. Similar to Figure 1a, the signal time-frequency signature cannot be recognized in this plot due to the low input SNR. When averaging the PWVD over all the $N_t N_r = 24$ transmit and receive antenna combinations, as shown in Figure 3b, the auto-terms are significantly enhanced and can be clearly identified in this plot. The difference between this plot and Figure 1b is also clear in the sense that the residual cross-terms are much higher. In this example, the spatial correlation

Table 2 Signal parameters of Example 2

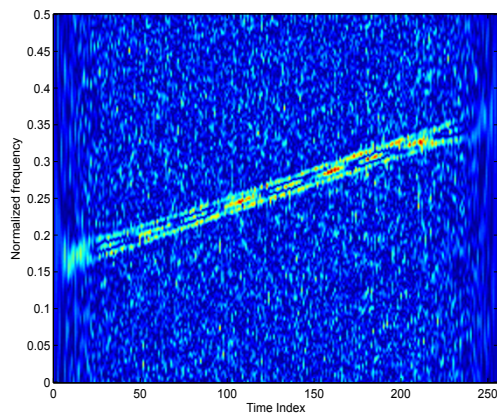
	Start freq.	End freq.	DOD (deg)	DOA (deg)
Target 1	0.15	0.35	10	15
Target 2	0.18	0.38	15	20



(a) single transmit-receive pair



(b) averaged over all virtual sensor pairs



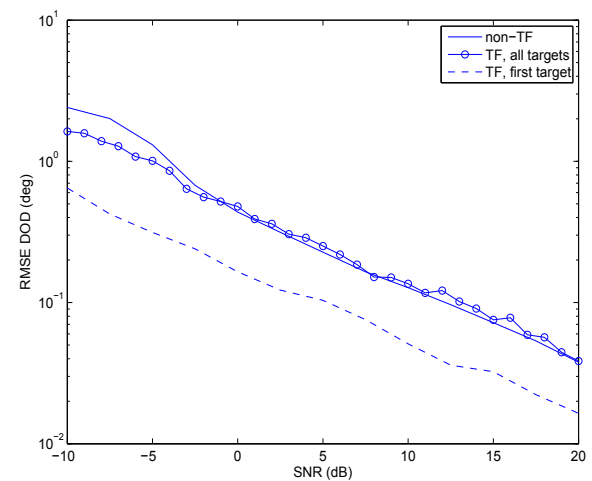
(c) averaged PWVD of signals with closer frequency difference of 0.2

Figure 3 Comparison of PWVD results. (a) Single transmit-receive pair; (b) averaged over all virtual sensor pairs; (c) averaged PWVD of signals with closer frequency difference of 0.2.

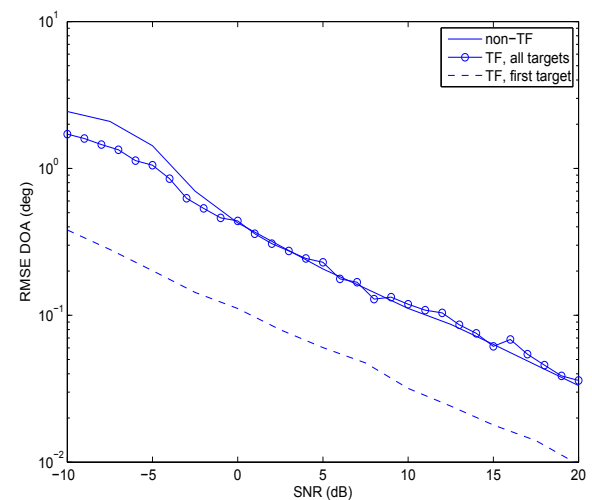
coefficient at the transmit array remains 0.956, whereas that at the receive array becomes 0.903 due to the closer angular separation between the two DOAs. This sets the overall spatial correlation coefficient of the MIMO array

to the high value of 0.863. To illustrate the effect of cross-terms on signals with close Doppler signature, Figure 3c plots the averaged PWVD for the chirp signals used in the first example.

In Figure 4, the RMSE of the DOD and DOA estimation results of the first target are compared for the same three different scenarios. When both signals are selected, the time-frequency ESPRIT-MUSIC still benefits from the SNR enhancement over low SNR regions. The performance of both DOD and DOA estimates is significantly improved through target discrimination by selecting only the first target. This improvement stems from overcoming the close angular separation of the



(a) DOD estimation



(b) DOA estimation

Figure 4 Comparison of RMSE performance. (a) DOD estimation; (b) DOA estimation.

targets at both the transmitter and receiver sides using time-frequency signature selections.

7. Conclusions

We have proposed the use of spatial time-frequency distributions (STFDs) for the joint DOD and DOA estimation of moving targets in a multiple-input multiple-output (MIMO) radar. Time-frequency analysis was applied to the target nonstationary Doppler data to enable signal enhancement and target discrimination. With MIMO configurations, the virtual array provided by the combination of different transmit and receive antenna pairs yields a significant number of virtual sensors. The virtually increased aperture empowers the STFD and allows for increased signal-to-noise ratio (SNR) and cross-term suppression, leading to reliable signal identification and selection. This, in turn, improves DOD/DOA estimation of weak targets with a low SNR. Most importantly, it was shown that the capability of discriminating targets with separable Doppler signatures in the time-frequency domain yields significant performance improvement of DOD/DOA estimation for targets with close angular separations.

Endnote

^aWhile joint block diagonalization may yield a better solution for subspace estimation from a set of STFD matrices defined in a region [13], we use weighted time-frequency averaging in this article for simplicity and intuitive description and implementations.

Acknowledgements

The study of Y. D. Zhang and M. G. Amin was supported in part by a subcontract with Dynetics, Inc. for research sponsored by the Air Force Research Laboratory (AFRL) under Contract FA8650-08-D-1303. Part of this study was presented at the 2011 IEEE International Conference on Acoustics, Speech, and Signal Processing, Prague, Czech Republic, May 2011 [27].

Author details

¹Center for Advanced Communications, Villanova University, Villanova, PA 19085, USA ²Air Force Research Laboratory, AFRL/RDMD, Dayton, OH 45433, USA

Competing interests

The authors declare that they have no competing interests.

Received: 16 November 2011 Accepted: 8 May 2012

Published: 8 May 2012

References

1. E Fisher, A Haimovich, R Blum, D Chizhik, L Cimini, R Valenzuela, MIMO radar: an idea whose time has come, in *Proc IEEE Radar Conf*, Philadelphia, PA, pp. 71–78 (2004)
2. Li J, Stoica P (eds.), *MIMO Radar Signal Processing* (Wiley-IEEE Press, New York, NY, 2009)
3. J Li, P Stoica, MIMO radar with colocated antennas. *IEEE Signal Process Mag.* **25**(2), 106–114 (2007)
4. C Duofang, C Baixiao, Q Guodong, Angle estimation using ESPRIT in MIMO radar. *Electron Lett.* **44**(2), 770–771 (2008). doi:10.1049/el:20080276
5. M Jin, G Liao, J Li, Joint DOD and DOA estimation for bistatic MIMO radar. *Signal Process.* **89**, 244–251 (2009). doi:10.1016/j.sigpro.2008.08.003
6. J Chen, H Gu, W Su, A new method for joint DOD and DOA estimation in bistatic MIMO radar. *Signal Process.* **90**, 714–719 (2010). doi:10.1016/j.sigpro.2009.08.003
7. ML Bencheikh, Y Wang, Joint DOD-DOA estimation using combined ESPRIT-MUSIC approach in MIMO radar. *Electron Lett.* **46**(2), 1081–1083 (2010)
8. NJ Willis, HD Griffiths, *Advances in Bistatic Radar*, (SciTech Publishing, Raleigh, NC, 2007)
9. Y Zhang, GJ Frazer, MG Amin, Concurrent operation of two over-the-horizon radars. *IEEE J Sel Topics Signal Process.* **1**(2), 114–123 (2007)
10. GJ Frazer, Y Abramovich, BA Johnson, Use of adaptive non-causal transmit beamforming in OTHR: experimental results, in *IEEE Radar Conf*, Rome, Italy, pp. 311–316 (2008)
11. VC Chen, H Ling, *Time-Frequency Transforms for Radar Imaging and Signal Analysis*, (Artech House, London, 2002)
12. A Belouchrani, M Amin, Blind source separation based on time-frequency signal representation. *IEEE Trans Signal Process.* **46**, 2888–2898 (1998). doi:10.1109/78.726803
13. A Belouchrani, MG Amin, Time-frequency MUSIC. *IEEE Signal Proc Lett.* **6**(2), 109–110 (1999)
14. AB Gershman, MG Amin, Wideband direction-of-arrival estimation of multiple chirp signals using spatial time-frequency distributions. *IEEE Signal Proc Lett.* **7**(2), 152–155 (2000)
15. Y Zhang, W Mu, MG Amin, Time-frequency maximum likelihood methods for direction finding. *J Franklin Inst.* **337**(2), 483–497 (2000)
16. Y Zhang, MG Amin, Spatial averaging of time-frequency distributions for signal recovery in uniform linear arrays. *IEEE Trans Signal Process.* **48**(2), 2892–2902 (2000)
17. MG Amin, Y Zhang, Direction finding based on spatial time-frequency distribution matrices. *Digital Signal Process.* **10**(2), 325–339 (2000)
18. A Belouchrani, K Abed-Meraim, MG Amin, AM Zoubir, Joint anti-diagonalization for blind source separation, in *Proc IEEE Int Conf Acoustics, Speech, and Signal Proc*, vol. 5. Salt Lake City, UT, pp. 2789–2792 (2001)
19. Y Zhang, W Mu, MG Amin, Subspace analysis of spatial time-frequency distribution matrices. *IEEE Trans Signal Process.* **49**(2), 747–759 (2001)
20. A Hassanien, AB Gershman, MG Amin, Time-frequency ESPRIT for direction-of-arrival estimation of chirp signals, in *Proc IEEE Sensor Array and Multichannel Signal Processing Workshop*, Rosslyn, VA, pp. 337–341 (2002)
21. W Mu, MG Amin, Y Zhang, Bilinear signal synthesis in array processing. *IEEE Trans Signal Process.* **51**(2), 90–100 (2003)
22. N Linh-Trung, A Belouchrani, K Abed-Meraim, B Boashash, Separating more sources than sensors using time-frequency distributions. *EURASIP J Appl Signal Process.* **2005**(2), 2828–2847 (2005)
23. Y Zhang, MG Amin, Blind separation of nonstationary sources based on spatial time-frequency distributions. *EURASIP J Applied Signal Processing.* **2006**, 13 (2006). Article ID 64785
24. MG Amin, Y Zhang, Spatial time-frequency distributions and DOA estimation, in *Classical and Modern Direction of Arrival Estimation*, ed. by Tuncer E, Friedlander B Academic Press, Burlington, MA, pp. 185–217 (2009)
25. MI Skolnik, *Introduction to Radar Systems*, 3rd edn. (Mc-Graw Hill, New York, NY, 2001)
26. L Cohen, *Time-Frequency Analysis*, (Prentice-Hall, Upper Saddle River, NJ, 1994)
27. YD Zhang, MG Amin, MIMO radar for direction finding with exploitation of time-frequency representations, in *Proc IEEE Int Conf Acoustics, Speech, and Signal Proc*, Prague, Czech Republic, pp. 2760–2763 (2011)

doi:10.1186/1687-6180-2012-102

Cite this article as: Zhang et al.: Joint DOD/DOA estimation in MIMO radar exploiting time-frequency signal representations. *EURASIP Journal on Advances in Signal Processing* 2012 **2012**:102.